Journal of Applied Sciences

ISSN 1812-5654

science alert

ANSInet
an open access publisher
http://ansinet.com

Journal of Applied Sciences 8 (12): 2258-2264, 2008
ISSN 1812-5654

Preparation and Characterization of Nanocomposite and Nanoporous Silk Fibroin Films

[1]Yaowalak Srisuwan, [1]Mangkorn Srisa-ard, [1]Chaiyasit Sittiwet, [1]Yodthong Baimark,
[2]Nual-Anong Narkkong and [3]Chirapha Butiman
[1]Department of Chemistry, Faculty of Science, Mahasarakham University, Mahasarakham 44150, Thailand
[2]Central Instrumentation Unit, Faculty of Science, Mahasarakham University, Mahasarakham 44150, Thailand
[3]Silk Innovation Center, Mahasarakham University, Mahasarakham 44150, Thailand

Abstract: Nanocomposite and nanoporous silk fibroin (SF) films were prepared by film casting of SF solution containing surfactant-free colloidal nanoparticles of methoxy poly (ethylene glycol)-*b*-poly (D, L-lactide) diblock copolymer (MPEG-*b*-PDLL). Self-condensation and nanophase separation of the nanoparticles from SF film matrix during film drying process gave nanopore structures. The colloidal nanoparticles were prepared in SF solution by modified-spontaneous emulsification solvent diffusion method without any surfactant. The interaction between SF and MPEG-*b*-PDLL in nanocomposite films was studied by Fourier transform infrared spectroscopy and thermogravimetry. The film transparency of SF nanocomposite films decreased as increasing the MPEG-*b*-PDLL ratio. Scanning Electron Microscopy (SEM) results indicated that the nanoparticle sizes in the films were in the range of 50-200 nm with spherical shape. Nanopore structures with pore size of less than 150 nm can be observed from SEM images of the film surface and cross-section. The nanopores are interconnected throughout the nanocomposite films. The number and size of nanoparticles and nanopores increased when the MPEG-*b*-PDLL ratio was increased.

Key words: Biodegradable polymers, nanoparticles, nanocomposite films, nanoporous films

INTRODUCTION

Silk fibroin (SF) is a biodegradable and biocompatible natural protein polymer created by the *Bombyx mori* silkworm (Altman *et al*., 2003) and has recently been extensively investigated as a biomaterial such as matrix for enzyme immobilization (Yoshimizu and Asakura, 1990), cell culture substrate (Minoura *et al*., 1995; Inouye *et al*., 1998), drug delivery system (Hanawa *et al*., 1995; Hofmann *et al*., 2006; Wang *et al*., 2007) and material for artificial skin (Yeo *et al*., 2000). The minimal inflammatory reactions *in vitro* and *in vivo* of SF film have been reported by Meinel *et al*. (2005). The SF has been electrospun to produce nanoporous membranes of SF nanofibers (Min *et al*., 2004; Jin *et al*., 2004). The nanoporous SF membranes have a wide distribution of pore sizes, high porosity and a high surface area to volume ratio, which are favorable features for cell attachment, proliferation and differentiation (Min *et al*., 2004).

The application of electrospinning technique for preparing nanofibers has greatly limited by higher-energy, expensive apparatus and difficult for large-scale preparation. From our previous work (Baimark *et al*., 2007a), the nanoporous chitosan films can be prepared as chitosan nanocomposite films with dispersing nanoparticles of methoxy poly(ethylene glycol)-*b*-poly (ε-caprolactone) (MPEG-b-PCL) into the chitosan film. The nanoparticles were self-condensed and nanophase separated from the chitosan film matrix.

MPEG-*b*-PDLL diblock copolymers have been synthesized to attain versatile biodegradable polymers having more water-absorbing capacity because of the inclusion of hydrophilic MPEG block within the relatively hydrophobic PDLL block (Lucke *et al*., 2000; Sun *et al*., 2004; Stefani *et al*., 2006). MPEG-*b*-PDLL have been used for the preparation of drug-loaded nanoparticles (Kim *et al*., 2005; Pierri and Avgoustakis, 2005; De Faria *et al*., 2005) with composed of the MPEG chains on the nanoparticle surfaces (Heald *et al*., 2002; Riley *et al*., 2003). Using of the modified-spontaneous emulsification solvent diffusion method (modified-SESD method) for preparing of surfactant-free MPEG-*b*-PDLL nanoparticles has been reported in our previous research (Baimark *et al*., 2007b). The use of a higher energy apparatus such as the homogenizer and sonicator in emulsion solvent evaporation method and high volume of water in dialysis method are avoided for this method. Hence, the large-scale preparation of the surfactant-free nanoparticles would be possible.

Corresponding Author: Yodthong Baimark, Department of Chemistry, Faculty of Science, Mahasarakham University, Mahasarakham 44150, Thailand Tel: +66-43-754246 Fax: +66-43-754246

In the present study, we adapted the modified-SESD method to prepare colloidal nanoparticles of MPEG-*b*-PDLL in SF aqueous solution without any surfactant before film casting. Then, the SF/MPEG-*b*-PDLL nanocomposite film was obtained following this procedure. Influence of SF/MPEG-*b*-PDLL ratios on the nanocomposite films was investigated and discussed. The intermolecular interaction between SF and MPEG-*b*-PDLL were analyzed by FT-IR spectroscopy and thermogravimetry. Scanning electron microscopy was used to observe morphology of film surface and cross-section. Film transparency was also determined by UV-Vis spectrophotometry.

MATERIALS AND METHODS

Materials: Silk fibroin (SF) aqueous solution was prepared by a chemical degummed method and dissolved before dialysis, respectively. Cocoons from *B. mori* were degummed by boiling twice in 0.5% Na_2CO_3 solution at 98-100°C for 30 min to remove sericin, then rinsed with distilled water and dried at room temperature. Degummed SF fibers were dissolved in the ternary solvent, $CaCl_2$-ethanol-water (mole ratio = 1:2:8), by stirring at 80°C for 2 h. The resulting SF solution was then dialyzed (cellulose tube) for 3 days against distilled water. The final concentration after dialysis was adjusted to 1% (w/v) against distilled water.

Methoxy poly(ethylene glycol)-*b*-poly(D, L-lactide) (MPEG-*b*-PDLL) was prepared as described in our previous work (Baimark *et al*., 2007b, c) by ring-opening polymerization of DLL at 130°C for 24 h using MPEG with molecular weight of 5,000 g mol^{-1} (Fluka, Germany) and stannous octoate (95%, Sigma, USA) as the initiating agents. The stannous octoate concentration was 0.02 mol%. As-polymerized MPEG-*b*-PDLL was purified by precipitation in n-hexane from chloroform solution before dried *in vacuo* at room temperature until constant weight. Number-average molecular weight and polydispersity of the MPEG-*b*-PDLL were determined from gel permeation chromatography as 73,600 and 1.88, respectively. All solvents and non-solvents, the analytical grade were used.

Methods

Preparation of nanocomposite and nanoporous SF films: The nanocomposite and nanoporous SF films with different SF/MPEG-*b*-PDLL composite ratios were prepared by film casting of SF aqueous solutions containing surfactant-free colloidal MPEG-*b*-PDLL nanoparticles. The colloidal nanoparticles were prepared by modified-SESD method in SF aqueous solution. Briefly, the MPEG-*b*-PDLL solution in mixture organic solvent of acetone/ethanol [3/3 (v/v)] was added drop-wise into SF solution with stirring at 600 rpm. The organic solvents were evaporated in fume hood for 6 h. Then, colloidal nanoparticles of MPEG-*b*-PDLL suspended in SF solution was obtained before poured on Petri dish and dried at 40°C for 24 h. The dried films were treated with 90% (v/v) methanol aqueous solution for 1 h before dried *in vacuo* at room temperature for one week. The SF/MPEG-*b*-PDLL ratios of the films were summarized in Table 1.

Table 1: Nanocomposite ratios, $T_{d,max}$ and T_{660} of SF, MPEG-*b*-PDLL and SF nanocomposite films

SF/MPEG-*b*-PDLL nanocomposite films (w/w)	1% (w/v) SF solution (mL)	MPEG-*b*-PDLL[a] (mg)	$T_{d,max}$[b] (°C)	T_{660}[c] (%)
20/0	20	-	312	74.5±3.6
20/1	20	0.01	317	70.0±3.7
20/2	20	0.02	318	60.4±4.5
20/3	20	0.03	338	32.8±4.7
0/20	-	0.20	312	95.2±1.0

[a]Amount of MPEG-*b*-PDLL dissolved in 2 mL [3/3 (v/v)] acetone/ethanol mixture solvent, [b]From DTG curves, [c]From UV-Vis spectrophotometry

Characterization of nanocomposite and nanoporous SF films: FT-IR spectra were collected by Fourier transform infrared (FT-IR) spectroscopy using Perkin-Elmer Spectrum GX FTIR spectrophotometer with air as the reference. The resolution of 4 cm^{-1} and 32 scans were chosen in this research.

Thermal decomposition behaviors were characterized by thermogravimetry (TG). The TA-Instrument TG SDT Q600 thermogravimetric analyzer was used to determine thermal decomposition profiles. For TG analysis, 10-20 mg sample was heated from 50 to 1,000°C at the heating rate of 20°C min^{-1} under nitrogen flow.

Film transparency was determined by measuring the percent transmittance at 660 nm using UV-Visible spectrophotometer (Lamda 25, Perkin-Elmer Instrument) as described by Rhim *et al*. (2006).

Film morphology was investigated by scanning electron microscopy (SEM) using JEOL JSM-6460LV SEM. The film was fractured in liquid nitrogen and coated with gold for enhanced conductivity before scan.

RESULTS AND DISCUSSION

FT-IR spectra: The structures of SF, MPEG-*b*-PDLL and SF nanocomposite films and the SF conformation transitions were investigated by FT-IR spectroscopy. The position of absorption bands indicated the conformation of SF. Figure 1 shows the FT-IR spectra of SF, MPEG-*b*-PDLL and SF nanocomposite films. The absorption bands of SF film in Fig. 1a at 1681 (amide 1), 1573 (amide 2) and 1234 cm^{-1} (amide 3) were assigned to the random coil structure of SF film. The absorption bands at 1615

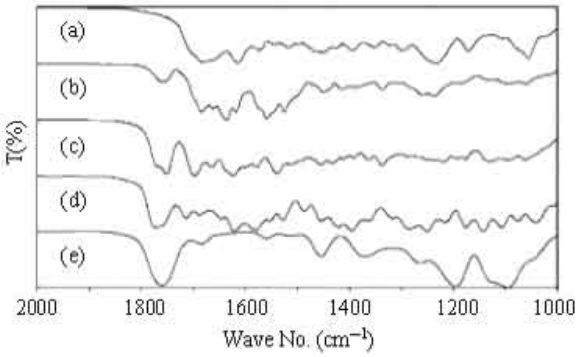

Fig. 1: FT-IR spectra of (a) SF, (b) 20/1 SF nanocomposite, (c) 20/2 SF nanocomposite, (d) 20/3 SF nanocomposite and (e) MPEG-*b*-PDLL films

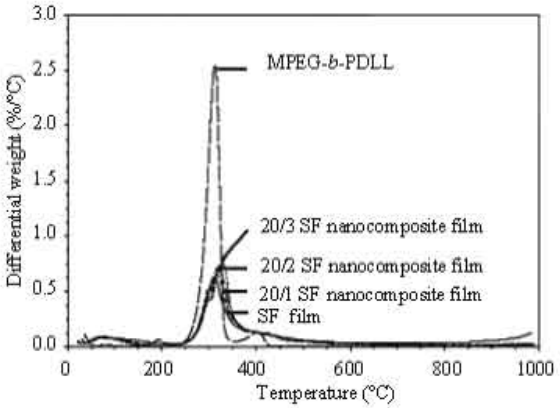

Fig. 2: DTG thermograms of SF, MPEG-*b*-PDLL and SF nanocomposite films

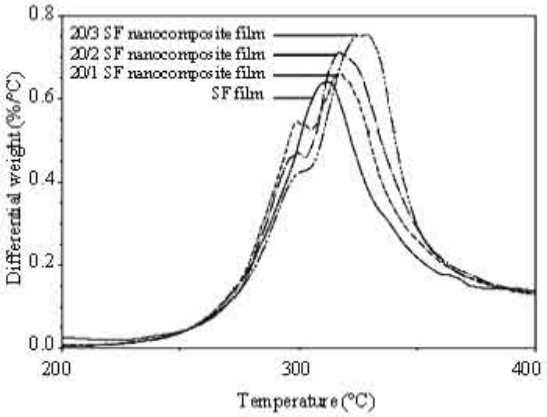

Fig. 3: Expanded DTG thermograms of SF and SF nanocomposite films

(amide 1) and 1521 cm^{-1} (amide 2) were indicated β-sheet structure of SF film (Wu *et al*., 2006). The splitting results of the amide bands indicated that the random coil and β-sheet structures were co-existed in the SF film after the methanol solution treatment. The MPEG-*b*-PDLL film was prepared by film casting of MPEG-*b*-PDLL solution in dichloromethane. The FT-IR spectrum of MPEG-*b*-PDLL film in Fig. 1e showed strong absorption band at 1760 cm^{-1}, attributed to the carbonyl stretching. The spectra of the SF nanocomposite films with SF/MPEG-*b*-PDLL composite ratios of 20/1, 20/2 and 20/3 (w/w) in Fig. 1b-d, respectively showed the bands of both SF and MPEG-*b*-PDLL characteristics. In parallel with hypothesis, the intensity of carbonyl bands of the SF nanocomposite films increased when the MPEG-*b*-PDLL ratio was increased.

In addition, the amide 1 and 2 bands for the SF nanocomposite films were shifted to higher wave number (Fig. 1a-d) indicated that the specific intermolecular interactions between SF and MPEG-*b*-PDLL in the nanocomposite films were existed. It was proposed that the formation of nanoparticles could induce the partial transformation of SF to a random coil conformation.

Thermal decomposition behaviors: The TG curve of MPEG-*b*-PDLL film shows a complete thermal decomposition at about 450°C. The TG curves of SF film shows residue weight approximately 30% at 1,000°C. Whereas, the TG profiles of SF nanocomposite films were strongly depended on the composite ratios (TG curves did not shown). The thermal decomposition behavior can be more clearly examined in detail from the differential thermogravimetric (DTG) curves, as shown in Fig. 2. From DTG curves, temperatures of maximum decomposition rate ($T_{d,max}$) are measured and summarized in Table 1. The DTG curves of SF and MPEG-*b*-PDLL films show same single $T_{d,max}$ at 312°C. All tested SF nanocomposite films showed a main single $T_{d,max}$. However, the $T_{d,max}$ of SF nanocomposite films were slightly higher than the SF film and increased as increasing the MPEG-*b*-PDLL ratio. The different thermal decomposition behaviors of SF and SF nanocomposite films were showed more clearly in expended DTG curves as shown in Fig. 3. The expanded DTG curves of SF and SF nanocomposite films presented lower shoulder peak at approximately 300°C due to the decomposition of lower interacted SF/MPEG-*b*-PDLL fraction. The $T_{d,max}$ of SF fraction slightly increased as increasing the MPEG-*b*-PDLL ratio. The results indicated that the MPEG-*b*-PDLL nanoparticles enhanced thermal decomposition stability of SF film matrix, which supported the existing of intermolecular interaction bonds between SF and MPEG-*b*-PDLL from FT-IR results.

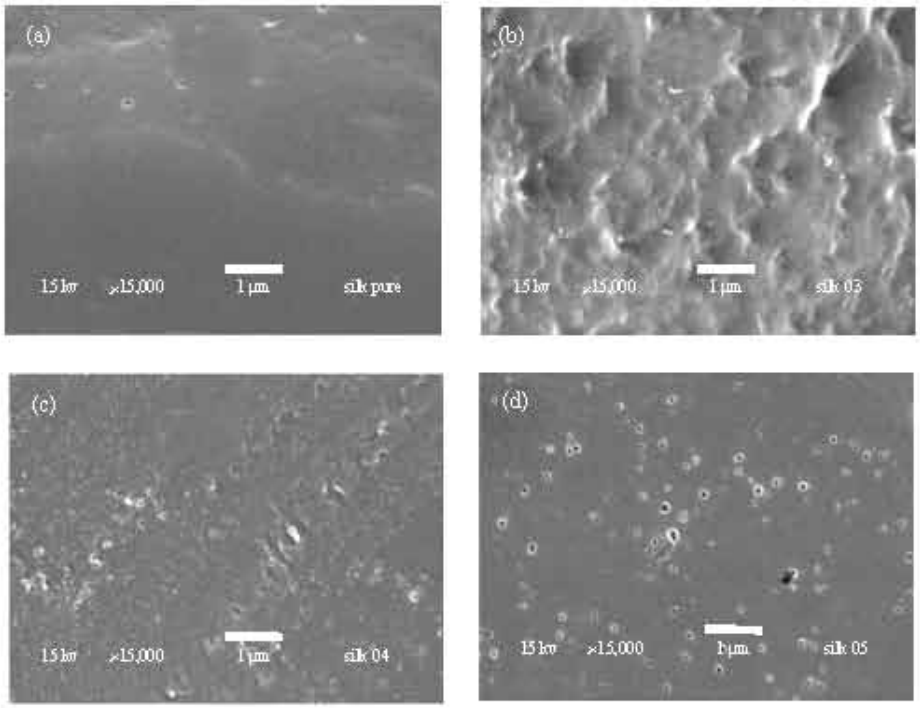

Fig. 4: SEM images of film surfaces of (a) SF, (b) 20/1 SF nanocomposite, (c) 20/2 SF nanocomposite and (d) 20/3 SF nanocomposite films (bar = 1 μm)

Film transparency: The MPEG-*b*-PDLL film was a clear transparent film. Similarly, the SF and SF nanocomposite films were also clear transparent films, with a slight yellowish and whiteness tint in the SF and SF nanocomposite films, respectively. Film transparency of SF, MPEG-*b*-PDLL and SF nanocomposite films was measured from % transmittance of the film at 660 nm (T_{660}). It was found that the MPEG-*b*-PDLL film is the highest transparent film due to its completely amorphous characteristic. Film transparency of the SF film was lower than the MPEG-*b*-PDLL film due to its crystallizable β-sheet form. It is interesting that the SF nanocomposites films containing MPEG-*b*-PDLL nanoparticles show more opaque than the SF film, as shown in Table 1. Rhim *et al*. (2006) have been reported that the transparency of chitosan films was not affected in significant value by nanocompositing with nanoparticles of sodium montmorillonite, organic modified montmorillonite and silver zeolite due to their have good dispersive and distributive through the chitosan film matrix. However, the transparency of chitosan film decreased as nanocompositing with silver nanoparticles due to its not good dispersive through the chitosan film matrix (Rhim *et al*., 2006). Then, decreasing the transparency of SF film as loading with MPEG-*b*-PDLL nanoparticles in this work may be due to the nanoparticles were not evenly dispersed throughout the SF film matrix. In addition, the film transparency was significantly decreased when the MPEG-*b*-PDLL ratio was increased. This was probably due to the nanoparticles of MPEG-*b*-PDLL were more aggregated through the SF film matrix as increasing the MPEG-*b*-PDLL ratio.

Film morphology: Thickness of the SF and its nanocomposite films was determined by SEM analysis. It was found to be in the range of 30-60 μm. Figure 4 shows the film surfaces morphology of SF and nanocomposite films. The MPEG-*b*-PDLL nanoparticles can be detected on the film surfaces of nanocomposite films with approximately 100 nm in sizes. The nanopores on film surfaces of nanocomposite films were found with sizes in the range of 50-200 nm. This due to self-condensed and phase separated of the MPEG-*b*-PDLL nanoparticles from the SF matrix during the drying process (Baimark *et al*., 2007a). The number and size of nanopores increased as increasing the MPEG-*b*-PDLL ratios.

Figure 5 shows the film cross-sections morphology of SF and nanocomposite films. The cross-sections of nanocomposite films were rougher than its surfaces. The nanoparticles and nanopores can be clearly observed that dispersed into the SF films in the ranges of 50-200 and less than 150 nm, respectively. Figure 6 shows expanded

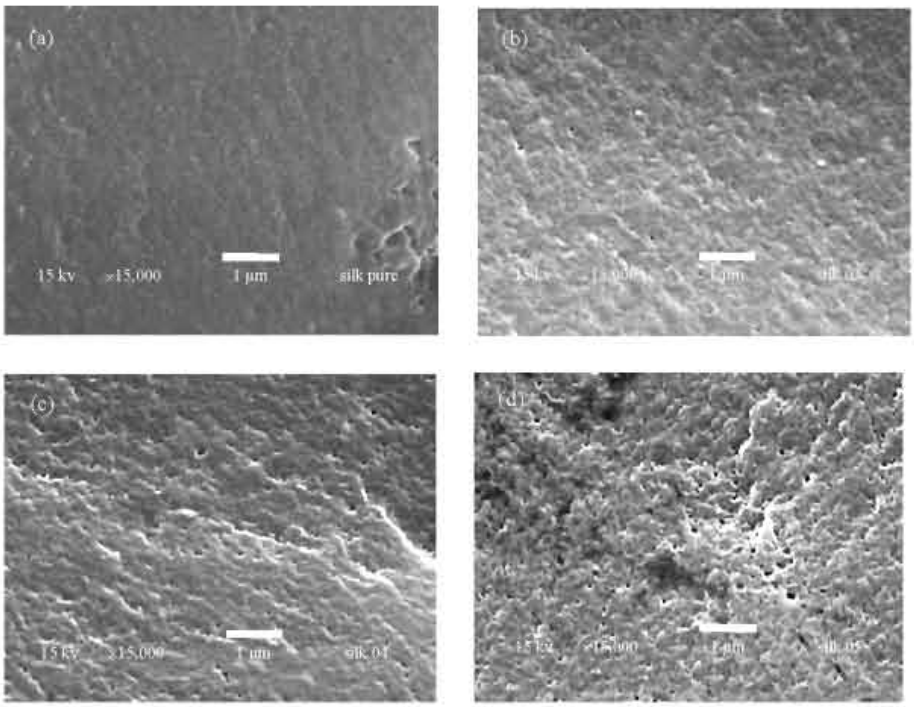

Fig. 5: SEM images of film cross-sections of (a) SF, (b) 20/1 SF nanocomposite, (c) 20/2 SF nanocomposite and (d) 20/3 SF nanocomposite films (bar = 1 μm)

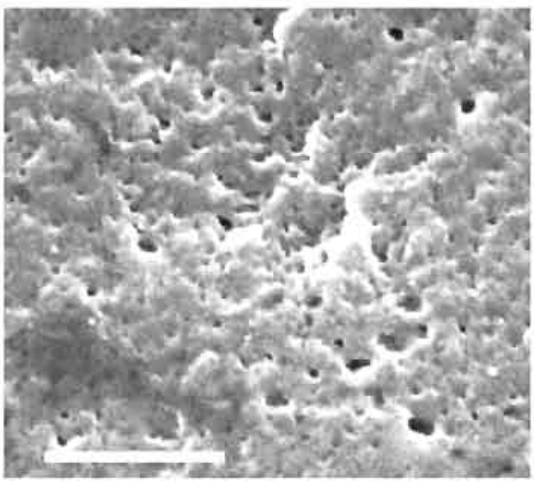

Fig. 6: Expanded SEM image of film cross-sections of 20/3 SF nanocomposite films (bar = 1 μm)

SEM image of cross-section of 20/3 SF nanocomposite film suggested that the nanocomposite film contain interconnected nanopores throughout the film. This indicated that the SF nanocomposite films consisted nanoporous structures. It should be noted that aggregated nanoparticles were also observed on the surface and the cross-section of SF film matrix suggested that the resulted SF nanocomposite films containing some aggregated nanoparticles with good distribution. This supports decreasing the film transparency of the SF nanocomposite films due to aggregating nanoparticles. Finally, this work indicated that the amorphous nanoparticles of MPEG-*b*-PDLL can also produce the nanoporous structure as the semi-crystalline nanoparticles of MPEG-b-PCL, as described in our previous work (Baimark *et al*., 2007a).

CONCLUSION

The SF nanocomposite films with different SF/MPEG-*b*-PDLL ratios were successfully prepared by film casting of the surfactant-free colloidal MPEG-*b*-PDLL nanoparticles suspended in SF aqueous solution. The intermolecular interactions between SF film matrix and MPEG-*b*-PDLL nanoparticles were investigated from FT-IR and DTG results. The SEM images showed the nanoparticles with spherical shape on film surfaces and cross-sections with nanoparticle sizes in the range of 50-200 nm. The SF nanocomposite films contained nanopore structure with the pore sizes of less than 150 nm. The number and size of nanoparticles and nanopores increased when the MPEG-*b*-PDLL ratios were increased. These nanoparticle-loaded SF nanocomposite

films with nanoporous structure might be of interested for cell or tissue engineering.

ACKNOWLEDGMENTS

The research was funded by the Research Development and Support Unit, Mahasarakham University, Mahasarakham, Thailand, fiscal year 2008 and the Center for Innovation in Chemistry: Postgraduate Education and Research Program in Chemistry (PERCH-CIC), Commission on Higher Education, Ministry of Education, Thailand.

REFERENCES

Altman, G.H., F. Diaz, C. Jakuba, T. Calabro, R.L. Horan, J. Chen, H. Lu, J. Richmond and D.L. Kaplan, 2003. Silk-based biomaterials. Biomaterials, 24: 401-416.

Baimark, Y., N. Niamsa, N. Morakot, J. Threeprom and Y. Srisuwan, 2007a. Preparation and morphology study of biodegradable chitosan/methoxy poly(ethylene glycol)-*b*-poly(ε-caprolactone) nanocomposite films. Int. J. Polym. Anal. Charat., 12: 457-467.

Baimark, Y., M. Srisa-ard, J. Threeprom and N. Narkkong, 2007b. Preparation nanoparticle colloids of methoxy poly(ethylene glycol)-*b*-poly(D,L-lactide): Effects of surfactant and organic solvent. Colloid Polym. Sci., 285: 1521-1525.

Baimark, Y., M. Srisa-ard, J. Threeprom, R. Molloy and W. Punyodom, 2007c. Synthesis and characterization of methoxy poly(ethylene glycol)-*b*-poly(D,L-lactide-co-glycolide-co-e-caprolactone) diblock copolymers: Effects of block lengths and compositions. E-Polymers, 138: 1-9.

De Faria, T.J., A.M. De Campos and E.L. Senna, 2005. Preparation and characterization of poly(D,L-lactide) (PLA) and poly(D,L-lactide)-poly(ethylene glycol) (PLA-PEG) nanocapsules containing antitumoral agent methotrexate. Macromol. Symp., 229: 228-233.

Hanawa, T., A. Watanabe, T. Tsuchiya, R. Ikoma, M. Hidaka and M. Sugihara, 1995. New oral dosage from for elderly patients: Preparation and characterization of silk fibroin gel. Chem. Pharm. Bull., 43: 284-288.

Heald, C.R., S. Stolnik, K.S. Kujawinski, C. De Matteis, M.C. Garnett, L. Illum, S.S. Davis, S.C. Purkiss, R.J. Barlow and P.R. Gellert, 2002. Poly(lactic acid)-poly(ethylene oxide) (PLA-PEG) nanoparticles: NMR studied of the central solidlike PLA core and the liquid PEG corona. Langmuir, 18: 3669-3675.

Hofmann, S., C.T. Wong Po Foo, F. Rossetti, M. Textor, G. Vunjak-Novakovic, D.L. Kaplan, H.P. Merkel and L. Meinel, 2006. Silk fibroin as an organic polymer for controlled drug delivery. J. Control. Release, 111: 219-227.

Inouye, K., M. Kurokawa, S. Nishikawa and M. Tsukada, 1998. Use of *Bombyx mori* silk fibroin as a substratum for cultivation of animal cells. J. Biochem. Biophys. Meth., 37: 159-164.

Jin, H.J., J. Chen, V. Karageorgiou, G.H. Altman and D.L. Kaplan, 2004. Human bone marrow stromal cell responses on electrospun silk fibroin mats. Biomaterials, 25: 1039-1047.

Kim, S.Y., Y.M. Lee and J.S. Kang, 2005. Indomethacin-loaded methoxy poly(ethylene glycol)/poly(D,L-lactide) amphiphilic diblock copolymeric nanospheres: Pharmacokinetic and toxicity studies in rodents. J. Biomed. Mater. Res., 74A: 581-590.

Lucke, A., J. Tebmar, E. Schnell, G. Schmeer and A. Gopferich, 2000. Biodegradable poly(D,L-lactic acid)-poly(ethylene glycol) monomethyl ether diblock copolymers: Structures and surface properties relevant to their use as biomaterials. Biomaterials, 21: 2361-2370.

Meinel, L., S. Hofmann, V. Karageorgiou, C. Kirker-Head, J. McCool, G. Gronowicz, L. Zichner, R. Langer, G. Vunjak-Novakovic and D.L. Kaplan, 2005. The inflammatory responses to silk films *in vitro* and *in vivo*. Biomaterials, 26: 147-155.

Min, B.M., G. Lee, S.H. Kim, Y.S. Nam, Y.S. Lee and W.H. Park, 2004. Electrospinning of silk fibroin nanofibers and its effect on the adhesion and spreading of normal human keratinocytes and fibroblasts *in vitro*. Biomaterials, 25: 1289-1297.

Minoura, N., S. Aiba, M. Higuchi, Y. Gotoh, M. Tsukada and Y. Imai, 1995. Attachment and growth of fibroblast cells on silk fibroin. Biochem. Biophys. Res. Commun., 208: 511-516.

Pierri, E. and K. Avgoustakis, 2005. Poly(lactide)-poly(ethylene glycol) micelles as a carrier for grisofulvin. J. Biomed. Mater. Res., 75A: 639-647.

Rhim J.W., S.I. Hong, H.M. Park and P.K.W. Ng, 2006. Preparation and characterization of chitosan-based nanocomposite films with antimicrobial activity. J. Agric. Food Chem., 54: 5814-5822.

Riley, T., C.R. Heald, S. Stolnik, M.C. Garnett, L. Illum and S.S. Davis, 2003. Core-shell structure of PLA-PEG nanoparticles used for drug delivery. Langmuir, 19: 8428-8435.

Stefani, M., J. Coudane and M. Vert, 2006. *In vitro* aging and degradation of PEG-PLA diblock copolymer based nanoparticles. Polym. Degrad. Stab., 9: 2554-2559.

Sun, J., Z. Xong, L. Yang, Z. Tang, X. Chen and X. Jing, 2004. Study on crystalline morphology of poly(L-lactide)-poly(ethylene glycol) diblock copolymer. Polymer, 45: 5969-5677.

Wang, X., E. Wenk, A. Matsumoto, L. Meinel, C. Li and D.L. Kaplan, 2007. Silk microspheres for encapsulation and controlled release. J. Control. Release, 117: 360-370.

Wu, Y., Q. Shen and S. Hu, 2006. Direct electrochemistry and electrocatalysis of home-protein in regenerated silk fibroin film. Anal. Chim. Acta., 558: 179-186.

Yeo, J.H., K.G. Lee, H.C. Kim, Y.L. Oh, A.J. Kim and S.Y. Kim, 2000. The effects of PVA/chitosan/fibroin (PCF)-blended spongy sheets on wound healing in rats. Biol. Pharm. Bull., 23: 1220-1223.

Yoshimizu, H. and T. Asakura, 1990. Preparation and characterization of silk fibroin powder and its application to enzyme immobilization. J. Applied Polym. Sci., 40: 127-134.